Current Research in Pharmacology and Drug Discovery 3 (2022) 100105

Contents lists available at ScienceDirect

Current Research in Pharmacology and Drug Discovery

journal homepage: www.journals.elsevier.com/current-research-in-pharmacology-and-drug-discovery

Hydroxycinnamic acid derivatives effect on hypercholesterolemia, comparison with ezetimibe: Permeability assays and FTIR spectroscopy on Caco-2 cell line

Asma Ressaissi [a,*], Maria Luísa M. Serralheiro [a,b]

[a] Universidade de Lisboa, Faculdade de Ciências, BioISI - Biosystems & Integrative Sciences Institute, Campo Grande, C8, 1749-016, Lisboa, Portugal
[b] Universidade de Lisboa, Faculdade de Ciências, Departamento de Química e Bioquímica, Campo Grande, 1749-016, Lisboa, Portugal

ARTICLE INFO

Keywords:
Cholesterol
Hydroxycinnamic acid derivatives
Ezetimibe
FTIR
Permeability
PCA

ABSTRACT

High blood cholesterol levels may increase the risk of developing atherosclerosis. Since intestinal cholesterol absorption plays a major role in maintaining total body cholesterol homeostasis, the aim of the present study was to compare the effect of ezetimibe and three hydroxycinnamic acid derivatives (rosmarinic acid, chlorogenic acid and m-coumaric acid) that are present in several medicinal plants on cholesterol absorption in the intestinal Caco-2 cells. In addition to the permeability assays, studies on alteration of the biochemical properties of Caco-2 cells under the effect of ezetimibe and hydroxycinnamic acid derivatives was evaluated using FTIR accompanied with multivariate analysis by PCA. The cholesterol permeability assays showed that these compounds could decrease cholesterol permeability with a percentage ranging from 76.98 to 96.6% with the highest inhibition for ezetimibe. whereas the FTIR studies didn't show similar changes between ezetimibe and the three hydroxycinnamic acid derivatives in protein and nucleic acids region, suggesting that these compounds have hypocholesterolemic effect. Nevertheless, each compound originated a different change on Caco-2 treated cells suggesting a different mode of action.

1. Introduction

Atherosclerosis is the major cause of myocardial infarctions and ischemic strokes. There is also general agreement that atherosclerosis, and thus coronary heart diseases, result from hypercholesterolemia. Although cholesterol is essential for mammalian cells, excess cholesterol is toxic and contributes to development of atherosclerotic vascular diseases (Hiebl et al., 2018; Yao et al., 2002). Cholesterol homeostasis is controlled mainly by endogenous synthesis, intestinal absorption, and hepatic excretion. An imbalance of these processes may lead to high cholesterol concentrations in the plasma, cholesterol accumulation in different tissues, and increased risk of atherosclerotic cardiovascular diseases (Park and Carr, 2013). Reduction in the intestinal absorption of dietary and biliary cholesterol can lead to the lowering of cholesterol levels. Recently, the use of drugs such as ezetimibe, a selective inhibitor of the transport of cholesterol, was one of the approaches to reduce serum cholesterol levels by decreasing cholesterol absorption in the small intestine which is a major interface in cholesterol uptake and excretion (Hiebl et al., 2020; Yoon et al., 2013). Caco-2 cells are mainly used for assessing the drug bioavailability, transport, and even metabolism in the intestine (van Breemen and Li, 2005), but they are also suitable for studying lipid and cholesterol homeostasis (Hiebl et al., 2020; Salvini et al., 2002). These cells are able to express membrane transporters; therefore, rendering them good models to study intestinal absorption and transport of natural products, as well as other processes that occur in the normal intestinal epithelium (Ming et al., 2011).

Due to the side effects of synthetic drugs, attention is now being directed to alternative medicines of plant origin (Loke et al., 2010). An important class of phenolic compounds such as hydroxycinnamic acid derivatives have attracted considerable interest in the past few years due to their known potential in diabetes and hyperlipidemia and they have been widely used as a template for the development of chemical entities with a potential therapeutic interest in human diseases (Arantes et al., 2016; Gungunes et al., 2018; Tsai et al., 2017). Many studies report a positive correlation between the consumption of medicinal plants rich in polyphenols (i.e., flavonoids) and a reduction in the risk of acquiring cardiovascular diseases, cancer, diabetes, obesity and degenerative diseases (Adaramoye et al., 2008; Rasouli et al., 2017;

* Corresponding author.
E-mail addresses: aressaissi@fc.ul.pt (A. Ressaissi), mlserralheiro@fc.ul.pt (M.L.M. Serralheiro).

https://doi.org/10.1016/j.crphar.2022.100105
Received 4 November 2021; Received in revised form 8 April 2022; Accepted 26 April 2022

Scalbert et al., 2005). These compounds are found in many plants and are abundant in fruits and vegetables. They have attracted much interest due to their preventive effects in cardiovascular disease and their ability to act on cholesterol homeostasis when present in the diet (Falé et al., 2013, 2014; Ressaissi et al., 2021; Scalbert et al., 2005). One of the techniques that has demonstrated its potential application in biomedical research, disease diagnosis, cellular biochemical studies, and therapeutic response monitoring is FTIR spectroscopy (Ukkonen et al., 2019). It is increasingly finding applications in the study of biochemical response of cell lines induced by drug treatment such as response of cells to mechanical stress, chemical stress, protein aggregation, cell attachment, cell death, cell differentiation and cell activation (Falé et al., 2014). This technique allows a rapid analysis of biochemical and structural changes in proteins, DNA, carbohydrates and lipids due to its high sensitivity in detecting modifications in the functional groups of the most important biomolecules. Its capacity to provide structure-specific spectra, containing all the vibrational modes of a sample, which gives a comprehensive data related with chemical and morphological information of the sample under analysis (Giorgini et al., 2017; Mihoubi et al., 2017). Due to their presence in herbal infusion and to their known potential on hypercholesterolemia, the objective of the present work was to study the bioavailability of ezetimibe (EZ) and hydroxycinnamic acid derivatives (m-coumaric acid (m-CA), rosamrinic acid (RA) and chlorogenic acid (ChA)) and their potential on lowering the permeability of cholesterol through Caco-2 cell monolayers. In addition, a comparison of the cellular response of Caco-2 cells exposed to (EZ) and the four hydroxycinnamic acid derivatives by analyzing the whole cell components using Fourier transform infrared spectroscopy (FTIR) was performed.

2. Material and methods

2.1. Chemicals

Trypsin, Dulbecco's modified Eagle medium (DMEM), glutamine, Pen-Strep (penicillin and streptomycin mixture), Phosphate-Buffered Saline (PBS) and fetal bovine serum (FBS) were bought from Lonza (Verviers, Belgium), 3-(4,5-Dimethylthiazol-2-yl)-2,5-diphenyltetrazolium bromide (MTT) from VWR International, m-coumaric acid (m-CA), rosmarinic acid (RA), chlorogenic acid (ChA) were bought from Sigma Aldrich, Barcelona, Spain and Ezetimibe commercial drug.

2.2. Cell culture

Caco-2, Human colorectal adenocarcinoma epithelial cell lines (ECACC 86010202) were cultured in DMEM supplemented with 10% FBS and 2 mM L-glutamine at 37 °C in an atmosphere with 5% CO_2 by seeding approx. 2×10^4 cells/cm^2. The medium was changed every 48–72 h, and cells were trypsinized before reaching confluence.

2.3. Cytotoxicity studies on Caco-2 cell line

Caco-2 cell line, Human colorectal adenocarcinoma epithelial cells were cultured in DMEM supplemented with 10% FBS and 2 mM L-glutamine at 37 °C in an atmosphere with 5% CO_2. Cells were passed every 48–72 h before reaching confluence. Cytotoxicity studies were performed using the MTT viability test (Ressaissi et al., 2017). Briefly, 2×10^4 cells were seeded in 96-well plates and incubated for 48 h at 37 °C in an atmosphere with 5% CO_2. Standards were dissolved in DMEM FBS free with different concentrations ranging from 0.025 to 1 mg/mL m-CA, RA and ChA and from 0.1 to 1 mM for EZ. The prepared solutions were incubated for 24 h in the same conditions before applying the MTT reagent. The assays were done in eight replicates for each concentration and the cell viability percentage was calculated by the following formula:

Viability (%) = [(Abs 595 – Abs 630 of sample)/(Abs 595 – Abs 630 of control)] × 100

2.4. Permeability assay

For transport and metabolism experiments, the cells (grown as previously described) were seeded at a density of 2–4 x 104 cells/cm2 in 12-well transwell plate inserts with 10.5 mm diameter, 0.4 μm pore size (BD Falcon™). The monolayers were formed after 16 days. The integrity of the monolayers was evaluated by measuring the transepithelial electrical resistance (TEER) with a Millicell ERS-2 V-Ohm Meter, from Millipore (Darmstadt, Germany). The membranes were considered fit when the TEER (electrical resistance) was higher than 250 Ω/cm2. The TEER was measured using a Millicell ERS-2 Volt-Ohm Meter, from Millipore (Darmstadt, Germany) before and after the assay. To start the assays solutions dissolved in DMEM containing 5 mM of cholesterol were applied into the transwell inserts (apical side of the cells) and DMEM was added to the plate well (basolateral side of the cells) (v/3v). After 24 h of incubation at 37 °C, 5% CO_2, the solutions in both sides of the cells were collected and analyzed by RP-HPLC-DAD (Falé et al., 2013). The percentage of permeation (%) was calculated as the amount transported divided by the initial amount in the apical chamber. The apparent permeability coefficients (Papp) were determined using the equation:

$$Papp = (dQ / dt) / (A \times C_0)$$

dQ/dt represents the rate of compound permeation to the basolateral side (mmol/s); A concerns to the surface area of the membrane (cm^2), and C_0 corresponds to the initial concentration of the compound.

2.5. FTIR analysis

The FTIR analysis were carried out as previously described (Ressaissi et al., 2020). HepG2 were maintained in T25 cell culture flasks using DMEM medium supplemented with 10% FBS and 2 mM L-glutamine, in a 5% CO_2 environment at 37 °C. The cells were trypsinized and harvested when they reached ~80% confluence. The cell suspension was diluted in medium to reach a cell density of $\sim 1.2 \times 10^6$ cell/mL. The resulting cell suspension was seeded directly onto CaF_2 windows and incubated overnight. The cells were treated with the phenolic compounds at concentration of 1 mM and Ezetimibe 100 μM (less than 40% toxicity) for 24 h. The spectra acquisitions were performed using Nicollet 6700 FT-IR apparatus from Thermo Electron Corporation®. All measurements were acquired with a spectral resolution of 4 cm^{-1} and a spectral range of 900–3000 cm^{-1}. Cell spectra were measured by averaging 128 scans. The OMINC software was used for acquisition and processing of spectra and FTIR spectra were normalized to Amide II band. For each assay, 4 replicates were performed.

2.6. Data analysis

All the data were expressed as mean ± standard deviation of at least four replicates. Analysis of variance (ANOVA) with $\alpha = 0.05$ (Turkey test), Peak area calculation, and second derivative methods were processed using OriginPro 2020b software. Spectra were smoothed by eight points Savitsky-Golay function. Principal Components Analysis (PCA) on the normalized spectra was carried out using OriginPro 2020b software. Spectra were truncated to 1300–950, 1500–1300, 1700–1600, and 3000-2800 cm^{-1} before PCA. The analysis was focused on the first two principal components (PC1 and PC2), as they accounted for more than 90% of the variances.

3. Results & discussion

3.1. Cytotoxicity studies on Caco-2 cell line

In this research, Caco-2 were subject to ezetimibe and phenolic acids treatment. The HCA derivatives and EZ were seen not to be toxic for the concentrations used. After being in contact with cells for 24 h, The percentage of toxicity for a concentration of 1 mg/mL of hydroxycinnamic acid derivatives was lower than 50% whereas EZ had an IC_{50} of 228.42 ± 29.5 μM (Table 1).

This low cytotoxicity showed by the 3 phenolic compounds allowed to study their bioavailability, their potential on lowering the permeability of cholesterol through Caco-2 cell monolayers and the changes in the cell macromolecular content and structure on Caco-2 cells using Infrared spectroscopy.

3.2. Permeability assays

The Caco-2 cell monolayer model is widely used to mimic the absorption and transport of drugs across the intestinal epithelial layer (Wang et al., 2020). The permeability of hydroxycinnamic acid derivatives and EZ in presence of cholesterol was studied by using the Caco-2 cell line differentiated as a monolayer, in a Transwell system. Phenolic acids and EZ were quantified in basolateral compartments after 24 h of incubation and the percentage of permeability and the apparent permeability coefficient (Papp) were calculated. The results are shown in Table 2.

In fact, in presence of cholesterol, all tested compounds could permeate the Caco-2 monolayer with a percentage ranging from 7.72 to 14.15 and a Papp values between 1.34 and 2.45 10^{-6} cm s^{-1} (Table 2). Ezetimibe showed the highest permeability. Moreover, the statistical analysis at 95% confidence level showed that ChA, m-CA and RA don't present significant difference between them, whereas EZ was statistically different when compared to RA, m-CA and ChA. These differences in bioavailability can be due to the interaction of these compounds with transport systems in intestinal cells, such as the monocarboxylic acid transporters (MCT), the ABC transporters P-glycoprotein (Pgp) and multidrug resistance proteins (MRP), which actively transport or inhibit by them (Falé et al., 2014).

According to Heinlein et al. (2014), substances with Papp values > 1.0×10^{-6} cm s^{-1} possess high absorption potential which mean that these compounds have a «high absorption potential». The obtained results showed that even with a diet rich in cholesterol, hydroxycinnamic acid derivatives and EZ have a high permeability and allow them to enter the blood stream and reach other organs such as the liver where they showed an effect cholesterol biosynthesis inhibition through the inhibition of the enzyme HMGR and the regulation of cholesterol transporter proteins responsible of cholesterol excretion (Arantes et al., 2016; Guedes et al., 2019; Ressaissi et al., 2017, 2020).

In addition to the bioavailability, the effect of hydroxycinnamic acid derivatives on cholesterol permeation was also evaluated in Caco-2 cell monolayers. The results are shown in Table 3.

Hydroxycinnamic acid derivatives and EZ were added simultaneously with cholesterol to the apical compartment of the transwells. After 24 h of being in contact with Caco-2 monolayer, the quantification of cholesterol on the basolateral compartment indicated that these compounds significantly decreased the permeation of cholesterol (Table 3).

Table 1
Cytotoxicity towards Caco-2 cell line of 1 mg/mL of hydroxycinnamic acid derivatives (%) and IC_{50} (μM) for Ezetemibe

	m-CA	ChA	RA	EZ
Caco-2 cell line	45.20 ± 1.44%	34.28 ± 0.8%	42.34 ± 3.54%	228.42 ± 329.5[a]

[a] IC_{50} (μM).

Table 2
Bioavailability of hydroxycinnamic acid derivatives and Ezetimibe through Caco-2 cells in presence of 5 mM of cholesterol (%).

	Bioavailability (%)	Papp (10^{-6} cm/s)
m-CA	7.72 ± 2.25[a]	1.34 ± 0.39[a]
ChA	7.95 ± 0.88[a]	1.38 ± 0.15[a]
RA	9.71 ± 2.36[a]	1.68 ± 0.41[a]
EZ	16.97 ± 0.26[b]	2.94 ± 0.04[b]

Table 3
Permeability of cholesterol through Caco-2 cells in the absence and presence of hydroxycinnamic acid derivatives and Ezetimibe (%).

	Cholesterol permeability	Decrease in cholesterol permeability
Cholesterol	19.1 ± 0.71	–
Cholesterol + EZ	0.64 ± 0.01[a]	96.60
Cholesterol + m-CA	4.25 ± 0.3[c]	77.70
Cholesterol + ChA	3.76 ± 0.5[b,c]	80.29
Cholesterol + RA	2.74 ± 0.01[b]	85.65

[a, b, c] Different letters mean significantly different at 0.05.

The obtained results showed that m-CA, ChA, RA and EZ decreased cholesterol permeability with a percentage ranging from 77.7 to 96.6%.

Although the presence of hydroxycinnamic acid derivatives decreased cholesterol permeation, the treatment with EZ showed the most important decrease in cholesterol permeability and it was statistically different from m-CA; ChA and RA at a critic level of 5%. Moreover, the statistical analysis at 95% confidence level showed that m-CA and RA present significant difference whereas ChA is not statistically different from m-CA and RA. For instance, cholesterol absorption in intestine is a multi-step process mediated by specific membrane proteins. The reduction in the permeation of cholesterol can be associated with the regulation of mRNA levels of Niemann-Pick Like 1 protein (NPC1L1) that promotes the transport of cholesterol inside the cells as well as ATP-binding cassette (ABC) proteins such as ABCG5 and ABCG8 which are cholesterol efflux transporters (Brown and Yu, 2009; Feng et al., 2017; Jia et al., 2011).

3.3. FTIR analysis

Fourier transform infrared spectroscopy (FTIR) has been shown to be a promising tool for identifying the mode of action of drugs. Small changes in cells' infrared spectra, induced by environmental conditions or drugs, may provide an accurate signature of the metabolic shift experienced by the cell as a response to change in the growth medium (Altharawi et al., 2020). The low cytotoxicity allowed to study the changes in the cells' macromolecular content and structure induced by ChA, m-CA, RA and EZ on Caco-2 cells using Infrared spectroscopy. As a

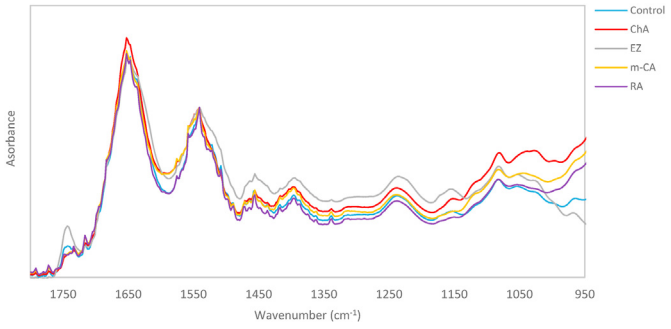

Fig. 1. Average of normalized spectra of Control and m-CA, ChA, RA, EZ treated cells in the spectral range 1800–950 cm^{-1}..

control we investigated the infrared response of untreated Caco-2 cell line (Fig. 1).

From the visual inspection of the spectra, it is evident that ChA, m-CA, RA and EZ induced significant spectral changes relatively to the control at different wavelengths in the spectral range 1800–950 cm^{-1} (Fig. 1). This Spectral range provides information about nucleic acids, proteins, and lipids (Ali et al., 2018).

To better investigate the spectral modifications arising from cell incubation with hydroxycinnamic acid derivatives (m-CA, ChA and RA) and EZ, we explored the infrared response between 1800 and 950 cm^{-1}, a very complex spectral range where carbohydrate and nucleic acid overlaps. The vibrations found between 1700 and 1600 cm^{-1} assigned to Amide I band, are directly related to the backbone conformation and can give information on the secondary structures in cell proteins. Absorbance at the wavenumbers 1652–1656 cm^{-1} are predominantly due to α-helical structures and the characteristic band for Random coil is located between 1646 and 1950 cm^{-1}, whereas wavenumbers between 1620 and 1642 cm^{-1} and 1667-1688 cm^{-1} are largely characteristic of β -structures (Ami et al., 2018; Yang et al., 2015).

The major bands in the 1300–950 cm^{-1} region are mainly due to carbohydrates (particularly glycogen) and phosphates associated with nucleic acids (Baker et al., 2014). The bands in the spectra at 965, 1081 and 1240 cm^{-1} are well-known DNA bands. The band near 965 cm^{-1} is originated from a C–C/C–O stretching vibration involving the characteristic deoxyribose and phosphate moiety of the DNA backbone whereas the bands at 1025 and 1154 cm^{-1} that is indicative of glycogen (Fale et al., 2015; Santos et al., 2018).

It can be seen in Fig. 2 that EZ and the hydroxycinnamic acid derivatives induced changes on the secondary structure of the cell protein. For instance, EZ induced more noticeable changes on α-helices/Random Coil and β-stuctures than m-CA, RA and ChA when compared to the untreated cells. The spectra was characterized by an increase in the component at ~1656 cm^{-1} which arises from α-helix for treated cells except with EZ, which showed a decrease. A decrease for random coil structures at 1650 cm^{-1} was also observed for treated cells, except for RA which showed an increase (Fig. 2). In the band area that can be assigned to β-sheets at ~1637 and 1683 cm^{-1}, an increase for treated cells with RA and a derease for treated cells with ChA and EZ was detected, whereas treated cells with m-CA didn't show any changes (Fig. 2). Based on this analysis, the changes in the absolute content of different secondary structure elements of treated cells with hydroxycinnamic acid derivatives and ezetimibe were observed.

Fig. 3, the second derivative of FTIR spectra for treated cells with ChA, m-CA, RA and EZ for the spectral range 1300–950 cm^{-1}, shows that the four phenolic acids induced changes in the main cell components but with different importance at different wavenumbers. In fact, relatively to the control, it can be seen a decrease in the intensity of the components at

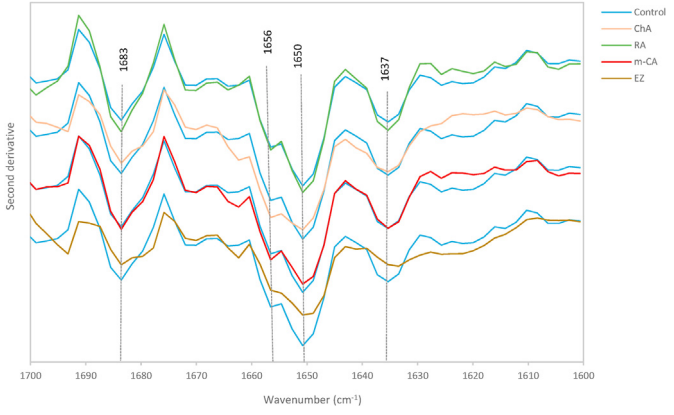

Fig. 2. Second derivative of Amide I of Control and m-CA, ChA, RA, EZ treated cells in the spectral range 1700–1600 cm^{-1}).

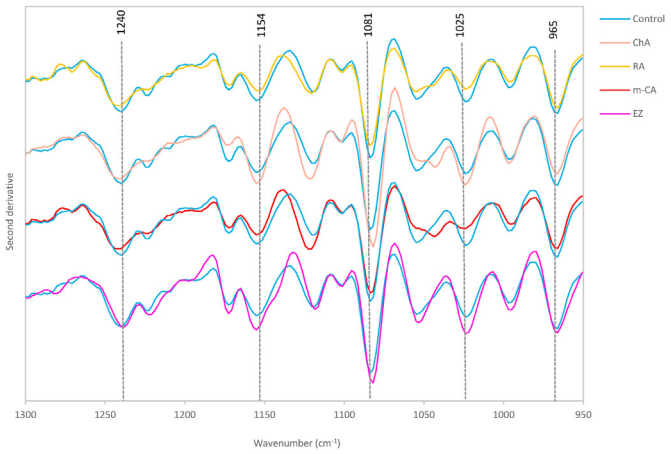

Fig. 3. Second derivative of FTIR spectra of Control and m-CA, ChA, RA, EZ treated cells in the spectral range 1300–1000 cm^{-1}.

1025 and 1154 cm^{-1} induced by m-CA and RA treatment whereas EZ and ChA induced an increase in those bands. Moreover, the bands at 965, 1081 and 1240 cm^{-1} showed an increase for EZ cell treated whereas a decrease induced by ChA, m-CA, RA at 965, 1081 and 1240 cm^{-1} was observed except ChA which showed an increase at 1081 cm^{-1}. These modifications can be attributed to structural changes in DNA volume or density.

Thus, the changes in the DNA and protein regions can be explained by the effect of these compounds on some transcriptional factors and the regulation mRNA and protein levels. The transcriptional control of many genes can be attributed to two families of transcription factors: the sterol regulatory element-binding proteins (SREBPs) (Horton et al., 2002) especially SREBP-2, which control the production of key enzymes in cholesterol biosynthesis, and the liver X receptors (LXRα and LXRβ) which regulate the expression of genes involved in cholesterol efflux, storage, catabolism, and elimination (Repa et al., 2002). Thus, transporter proteins expression and their activity is regulated by transcriptional as well as post-transcriptional mechanisms. For instance, it is known that EZ, drug used to treat hypercholesterolemia, inhibits Niemann-Pick C1-like 1 (NPC1L1) and mediates cellular cholesterol uptake (Feng et al., 2017; Nakano et al., 2020). Furthermore, in the intestine, Liver X Receptors LXRs limits cholesterol absorption by downregulating NPC1L1 (Duval et al., 2006). Moreover, it has been shown that in the intestine, activation of LXR enhances fecal sterol excretion via upregulation of the transporter heterodimer ABCG5/G8 (Hiebl et al., 2018).

3.4. Principal component analysis of FTIR spectral data

To further clarify differences between spectra of cells exposed to dissimilar conditions, and to identify main sources of variation, the previous analysis was complemented by Principal Component Analysis (PCA). Spectra were separated in two regions for PCA, corresponding to characteristic vibrations of different cell components. PCA of control and treated cells are shown in Fig. 4. The analysis by regions reduces artifacts caused by interference of unrelated compounds.

As it can be seen in Fig. 4, the score plots of PC1 versus PC2 clearly separated hydroxycinnamic acid derivatives treated cells from ezetimibe treated cells for the two regions 1300–950, and 1700–1600 cm^{-1} whereas PC1 versus PC2 did not separate the hydroxycinnamic acid derivatives very well.

The region 1300–950 cm^{-1} showed a dominating PC1 explaining 74.3% of the variation in the set of spectra, and PC2 (24.8%) which gave a clear separation of hydroxycinnamic acid derivatives treated cells and EZ treated cells (Fig. 4a). For instance, PC1 did not highlight changes at 1300-950 cm^{-1} whereas PC2 explaining 24.5% of the variance

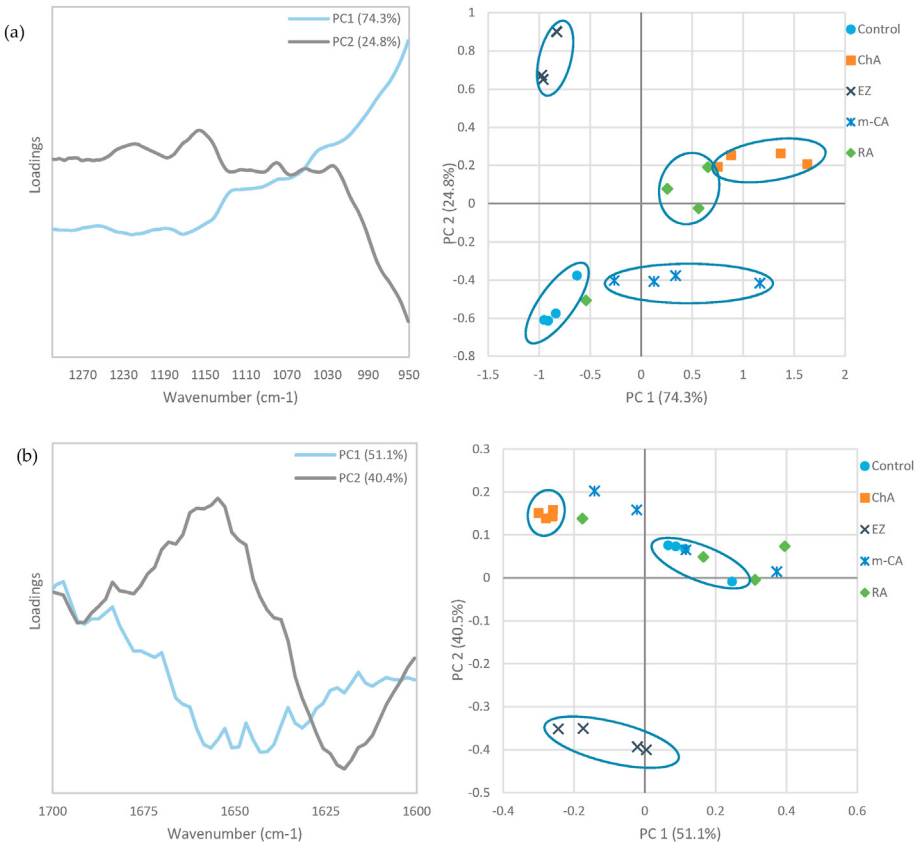

Fig. 4. Analysis of FTIR spectra of Control and m-CA, ChA, RA, EZ treated cells with PCA. PC loadings and score scatter plots of the corresponding PC1 and PC2. Spectral regions were considered for analysis, (a) 1300–950 cm^{-1}, (b) 1700–1600 cm^{-1}.

highlighted changes with positive loadings at 1025, 1081 and 1154 cm^{-1}. The score plot of PC1 versus PC2 showed a grouping of compounds with similar pattern. Control cells and treated cells form discrete clusters, presenting higher amount of glycogen and *vsym/asym* PO_2- for EZ treated cells. However, PC1 (74.5%) separated control from hydroxycinnamic acid derivatives treated cells with higher scores for hydroxycinnamic acid derivatives treated cells which were mainly separated among PC2 (24.5%).

In the region 1700–1600 cm^{-1}, which is generally attributed to the amide I band associated with α-helix β-structures and Random coil secondary structure (Ami et al., 2018), PC1 (51.1%) and PC2 (40.4%) highlighted changes with negative loadings at 1650 and 1656 cm^{-1}. In addition, PC2 loadings plot showed positive loadings at 1637 and 1683 cm^{-1}. The scores scatter plot PC1 vs. PC2 shows a clear separation of cell groups along the PC1 and PC2. PC2 explaining 40.0% of variance has clearly separated treated cells with hydroxycinnamic acid derivatives and EZ, however the separation between hydroxycinnamic acid derivatives treated cells was not clear except ChA treated cells which formed a cluster (Fig. 4b).

4. Conclusion

Although the combined FTIR spectroscopy with principal component analysis has shown that hydroxycinnamic acids and ezetimibe have a different mode of action on Caco-2 cells component, these compounds showed their ability to lower cholesterol uptake through caco-2 cell lines with small difference when compared to ezetimibe. In addition, the bioavailability assays demonstrated that even with a diet rich in cholesterol, hydroxycinnamic acids derivatives could decrease the cholesterol intestinal permeability and permeate the intestinal barrier to reach other organs. These findings allow to suggest that herbal infusions containing these compounds might be used as cholesterol reducing agents and by the way avoiding the side effects of Ezetimibe.

Funding

This research was supported by the Portuguese Foundation for Science and Technology, FCT, through the Research Unit grant UID/MULTI/04046/2019 to BioISI and FCT project PTDC/BIA-BQM/28355/2017.

CRediT authorship contribution statement

Asma Ressaissi: Conceptualization, Methodology, Investigation, Software, Data curation, Validation, Writing – original draft. **Maria Luísa M. Serralheiro:** Conceptualization, Validation, Writing – review & editing, Supervision.

Declaration of competing interest

The authors declare that they have no known competing financial interests or personal relationships that could have appeared to influence the work reported in this paper.

References

Adaramoye, O., Akintayo, O., Achem, J., Fafunso, M.a., 2008. P34 lipid-lowering effect of methanolic extract of Vernonia Amygdalina leaves in rats fed on high cholesterol diet. Vasc. Health Risk Manag. 4, 235–241. https://doi.org/10.2147/vhrm.2008.04.01.235.

Ali, M., Rakib, F., Nischwitz, V., Ullah, E., Mall, R., Shraim, A.M., Ahmad, M.I., Ghouri, Z.K., McNaughton, D., Küppers, S., Ahmed, T., Al-Saad, K., 2018. Application of FTIR and LA-ICPMS spectroscopies as a possible approach for biochemical analyses of different rat brain regions. Appl. Sci. 8. https://doi.org/10.3390/app8122436.

Altharawi, A., Rahman, K.M., Chan, K.L.A., 2020. Identifying the responses from the estrogen receptor-expressed MCF7 cells treated in anticancer drugs of different

modes of action using live-cell FTIR spectroscopy. ACS Omega 5, 12698–12706. https://doi.org/10.1021/acsomega.9b04369.
Ami, D., Mereghetti, P., Leri, M., Giorgetti, S., Natalello, A., Doglia, S.M., Stefani, M., Bucciantini, M., 2018. A FTIR microspectroscopy study of the structural and biochemical perturbations induced by natively folded and aggregated transthyretin in HL-1 cardiomyocytes. Sci. Rep. 8, 1–15. https://doi.org/10.1038/s41598-018-30995-5.
Arantes, A.A., Falé, P.L., Costa, L.C.B., Pacheco, R., Ascensão, L., Serralheiro, M.L., 2016. Inhibition of HMG-CoA reductase activity and cholesterol permeation through Caco-2 cells by caffeoylquinic acids from Vernonia condensata leaves. Brazilian J. Pharmacogn. 26, 738–743. https://doi.org/10.1016/j.bjp.2016.05.008.
Baker, M.J., Trevisan, J., Bassan, P., Bhargava, R., Butler, H.J., Dorling, K.M., Fielden, P.R., Fogarty, S.W., Fullwood, N.J., Heys, K.A., Caryn Hughes, C., Lasch, P., Martin-Hirsch, Pierre L., Obinaju, Blessing, Sockalingum, Ganesh D., Sulé-Suso, Josep, Strong, Rebecca J., Walsh, Michael J., Wood, Bayden R., Gardner, Peter, Martin, Francis L., 2014. Using Fourier transform IR spectroscopy to analyze biological materials. Nat. Protoc. 9, 1771–1791. https://doi.org/10.1007/s13398-014-0173-7.2.
Brown, J.M., Yu, L., 2009. Opposing gatekeepers of apical sterol transport: Niemann-Pick C1-like 1 (NPC1L1) and ATP-binding cassette transporters G5 and G8 (ABCG5/ABCG8). Immunol. Endocr. Metab. Agents Med. Chem. 9, 18–29. https://doi.org/10.2174/187152209788009797.
Duval, C., Touche, V., Tailleux, A., Fruchart, J.C., Fievet, C., Clavey, V., Staels, B., Lestavel, S., 2006. Niemann-Pick C1 like 1 gene expression is down-regulated by LXR activators in the intestine. Biochem. Biophys. Res. Commun. 340, 1259–1263. https://doi.org/10.1016/j.bbrc.2005.12.137.
Falé, P., Ferreira, C., Maruzzella, F., Helena Florêncio, M., Frazão, F.N., Serralheiro, M.L.M., 2013. Evaluation of cholesterol absorption and biosynthesis by decoctions of Annona cherimola leaves. J. Ethnopharmacol. 150, 718–723. https://doi.org/10.1016/j.jep.2013.09.029.
Falé, P., Ferreira, C., Rodrigues, A., Frazão, F., Serralheiro, M., 2014. Studies on the molecular mechanism of cholesterol reduction by Fraxinus angustifolia, Peumus boldus, Cynara cardunculus and Pterospartum tridentatum. J. Med. Plants Res. 8, 9–17. https://doi.org/10.5897/JMPR2013.5273.
Fale, P.L., Altharawi, A., Chan, K.L.A., 2015. In situ Fourier transform infrared analysis of live cells' response to doxorubicin. Biochim. Biophys. Acta Mol. Cell Res. 1853, 2640–2648. https://doi.org/10.1016/j.bbamcr.2015.07.018.
Feng, D., Zou, J., Zhang, S., Li, X., Li, P., Lu, M., 2017. Bisphenol A promotes cholesterol absorption in Caco-2 cells by up-regulation of NPC1L1 expression. Lipids Health Dis. 16, 2. https://doi.org/10.1186/s12944-016-0395-0.
Giorgini, E., Sabbatini, S., Conti, C., Rubini, C., Rocchetti, R., Fioroni, M., Memè, L., Orilisi, G., 2017. Fourier Transform Infrared Imaging analysis of dental pulp inflammatory diseases. Oral Dis. 23, 484–491. https://doi.org/10.1111/odi.12635.
Guedes, L., Reis, P.B.P.S., Machuqueiro, M., Ressaissi, A., Pacheco, R., Serralheiro, M.L., 2019. Bioactivities of Centaurium erythraea (Gentianaceae) Decoctions: antioxidant activity, enzyme inhibition and docking studies. Molecules 24. https://doi.org/10.3390/molecules24203795.
Gungunes, C.D., Alpsoy, L., Baykal, A., Nawaz, M., Akal, Z.Ü., 2018. The effect of folic acid- and caffeic acid-functionalized SPION on different cancer cell lines. J. Supercond. Nov. Magnetism 31, 3579–3588.
Heinlein, A., Metzger, M., Walles, H., Buettner, A., 2014. Transport of hop aroma compounds across Caco-2 monolayers. Food Funct. 5, 2719–2730. https://doi.org/10.1039/c3fo60675a.
Hiebl, V., Ladurner, A., Latkolik, S., Dirsch, V.M., 2018. Natural products as modulators of the nuclear receptors and metabolic sensors LXR. FXR and RXR. Biotechnol. Adv. 36, 1657–1698. https://doi.org/10.1016/j.biotechadv.2018.03.003.
Hiebl, V., Schachner, D., Ladurner, A., Heiss, E.H., Stangl, H., Dirsch, V.M., 2020. Caco-2 cells for measuring intestinal cholesterol transport-Possibilities and limitations. Biol. Proced. Online 22, 1–18. https://doi.org/10.1186/s12575-020-00120-w.
Horton, J.D., Goldstein, J.L., Brown, M.S., 2002. SREBPs: activators of the complete program of cholesterol and fatty acid synthesis in the liver. J. Clin. Invest. 109, 1125–1131. https://doi.org/10.1172/JCI200215593. Lipid.
Jia, L., Betters, J.L., Yu, L., 2011. Niemann-Pick C1-Like 1 (NPC1L1) protein in intestinal and hepatic cholesterol transport. Annu. Rev. Physiol. 73, 239–259. https://doi.org/10.1146/annurev-physiol-012110-142233.
Loke, W.M., Proudfoot, J.M., Hodgson, J.M., McKinley, A.J., Hime, N., Magat, M., Stocker, R., Croft, K.D., 2010. Specific dietary polyphenols attenuate atherosclerosis in apolipoprotein e-knockout mice by alleviating inflammation and endothelial dysfunction. Arterioscler. Thromb. Vasc. Biol. 30, 749–757. https://doi.org/10.1161/ATVBAHA.109.199687.
Mihoubi, W., Sahli, E., Gargouri, A., Amiel, C., 2017. FTIR spectroscopy of whole cells for the monitoring of yeast apoptosis mediated by p53 over-expression and its suppression by Nigella sativa extracts. PLoS One 12, 1–16. https://doi.org/10.1371/journal.pone.0180680.
Ming, X., Knight, B.M., Thakker, D.R., 2011. Vectorial transport of fexofenadine across caco-2 cells: involvement of apical uptake and basolateral efflux transporters. Mol. Pharm. 8, 1677–1686. https://doi.org/10.1021/mp200026v.
Nakano, T., Inoue, I., Takenaka, Y., Ito, R., Kotani, N., Sato, S., Nakano, Y., Hirasaki, M., Shimada, A., Murakoshi, T., 2020. Ezetimibe impairs transcellular lipid trafficking and induces large lipid droplet formation in intestinal absorptive epithelial cells. Biochim. Biophys. Acta Mol. Cell Biol. Lipids 1865, 158808. https://doi.org/10.1016/j.bbalip.2020.158808.
Park, Y., Carr, T.P., 2013. Unsaturated fatty acids and phytosterols regulate cholesterol transporter genes in Caco-2 and HepG2 cell lines. Nutr. Res. 33, 154–161. https://doi.org/10.1016/j.nutres.2012.11.014.
Rasouli, H., Farzaei, M.H., Khodarahmi, R., 2017. Polyphenols and their benefits: a review. Int. J. Food Prop. 20, 1700–1741. https://doi.org/10.1080/10942912.2017.1354017.
Repa, J.J., Berge, K.E., Pomajzl, C., Richardson, J.A., Hobbs, H., Mangelsdorf, D.J., 2002. Regulation of ATP-binding cassette sterol transporters ABCG5 and ABCG8 by the liver X receptors α and β. J. Biol. Chem. 277, 18793–18800. https://doi.org/10.1074/jbc.M109927200.
Ressaissi, A., Attia, N., Falé, P.L., Pacheco, R., Victor, B.L., Machuqueiro, M., Serralheiro, M.L.M., 2017. Isorhamnetin derivatives and piscidic acid for hypercholesterolemia: cholesterol permeability, HMG-CoA reductase inhibition, and docking studies. Arch Pharm. Res. (Seoul) 40, 1278–1286. https://doi.org/10.1007/s12272-017-0959-1.
Ressaissi, A., Attia, N., Pacheco, R., Falé, P.L., Serralheiro, M.L.M., 2020. Cholesterol transporter proteins in HepG2 cells can be modulated by phenolic compounds present in Opuntia ficus-indica aqueous solutions. J. Funct.Foods 64, 103674. https://doi.org/10.1016/j.jff.2019.103674.
Ressaissi, A., Pacheco, R., Serralheiro, M.L.M., 2021. Molecular-level changes induced by hydroxycinnamic acid derivatives in HepG2 cell line: comparison with pravastatin. Life Sci. 283, 119846. https://doi.org/10.1016/j.lfs.2021.119846.
Salvini, S., Charbonnier, M., Defoort, C., Alquier, C., Lairon, D., 2002. Functional characterization of three clones of the human intestinal Caco-2 cell line for dietary lipid processing. Br. J. Nutr. 87, 211–217. https://doi.org/10.1079/bjn2001507.
Santos, F., Magalhães, S., Henriques, M.C., Fardilha, M., Nunes, A., 2018. Spectroscopic features of cancer cells: FTIR spectroscopy as a tool for early diagnosis. Curr. Metabolomics 6, 103–111. https://doi.org/10.2174/2213235X06666180521084551.
Scalbert, A., Manach, C., Morand, C., Rémésy, C., Jiménez, L., 2005. Dietary polyphenols and the prevention of diseases. Crit. Rev. Food Sci. Nutr. 45, 287–306. https://doi.org/10.1080/1040869059096.
Tsai, T.H., Yu, C.H., Chang, Y.P., Lin, Y.T., Huang, C.J., Kuo, Y.H., Tsai, P.J., 2017. Protective effect of caffeic acid derivatives on tert-butyl hydroperoxide-induced oxidative hepato-toxicity and mitochondrial dysfunction in HepG2 cells. Molecules 22. https://doi.org/10.3390/molecules22050702.
Ukkonen, H., Vuokila, S., Mikkonen, J.J.W., Dekker, H., Schulten, E.A.J.M., Bloemena, E., Koistinen, A., Valdez, T.A., Kullaa, A.M., Singh, S.P., 2019. Biochemical changes in irradiated oral mucosa : a FTIR spectroscopic study. Biosensors 9, 12. https://doi.org/10.3390/bios9010012.
van Breemen, R.B., Li, Y., 2005. Caco-2 cell permeability assays to measure drug absorption. Expet Opin. Drug Metabol. Toxicol. 1, 175–185. https://doi.org/10.1517/17425255.1.2.175.
Wang, Y., Bai, X., Hu, B., Xing, M., Cao, Q., Ji, A., Song, S., 2020. Transport mechanisms of polymannuronic acid and polyguluronic acid across caco-2 cell monolayers. Pharmaceutics 12. https://doi.org/10.3390/pharmaceutics12020167.
Yang, H., Yang, S., Kong, J., Dong, A., Yu, S., 2015. Obtaining information about protein secondary structures in aqueous solution using Fourier transform IR spectroscopy. Nat. Protoc. 10, 382–396. https://doi.org/10.1038/nprot.2015.024.
Yao, L., Heubi, J.E., Buckley, D.D., Fierra, H., Setchell, K.D.R., Granholm, N. a, Tso, P., Hui, D.Y., Woollett, L. a, 2002. Separation of micelles and vesicles within lumenal aspirates from healthy humans: solubilization of cholesterol after a meal. J. Lipid Res. 43, 654–660. https://doi.org/10.1016/S0022-2275(20)31496-6.
Yoon, H.S., Ju, J.H., Kim, H.N., Park, H.J., Ji, Y., Lee, J.E., Shin, H.K., Do, M.S., Holzapfel, W., 2013. Reduction in cholesterol absorption in Caco-2 cells through the down-regulation of Niemann-Pick C1-like 1 by the putative probiotic strains Lactobacillus rhamnosus BFE5264 and Lactobacillus plantarum NR74 from fermented foods. Int. J. Food Sci. Nutr. 64, 44–52. https://doi.org/10.3109/09637486.2012.706598.